SAND2015-0493PE

Exceptional service in the national interest

Sandia National Laboratories

Enabling Technologies for Single Electron Spin Resonance in Silicon

Stephen M. Carr

Sandia National Laboratories

Center for Quantum Information and Control (CQuIC) Seminar

University of New Mexico

January 29, 2015

Acknowledgements

Quantum Information Science and Technology (QIST) at Sandia National Laboratories

Principal Investigator: Malcolm Carroll

ESR Fabrication:

- L.A. Tracy
- N. Bishop
- T. Pluym
- J. Wendt
- G. Ten Eyck
- M.P. Lilly

ESR Microwave Design and Cryogenic Hardware:

- J. Borchardt
- S.M. Carr

ESR Measurement:

- D.R. Luhman
- K. Nguyen
- L.A. Tracy
- M.P. Lilly

Joint Research Efforts with the External Community

- Center for Quantum Information and Control (CQuIC) at University of New Mexico (M.J. Curry and I. Deutsch)
- Australian Centre for Quantum Computing and Communication Technology (CQCCT) (A. Dzurak, L. Hollenberg, D. Jamieson, A. Morello, S. Rogge, M. Simmons)
- Princeton University (S. Lyon)
- NIST (N. Zimmerman)
- U. Maryland (S. Das Sarma)
- National Research Council (A. Sachrajda)
- U. Sherbrooke (P. Harvey-Collard, C. Bureau-Oxton, M. Pioro-Ladriere)
- Purdue University (G. Klimeck & R. Rahman)
- U. Wisconsin (M. Eriksson, M. Friesen)

Outline

- Physical Implementations of Qubits
- Silicon-Based Spin Qubits
- Sandia Silicon Device Description and Qubit Definition
- Description of the Cryogenic Microwave Engineering Challenge
- Electromagnetic Field Simulation Description and Results
- Experimental Demonstration of Coherent Rabi Oscillations of a Single Electron Spin in Silicon
- Comparison Between Experimental Data and Simulation

Physical Implementations of Qubits

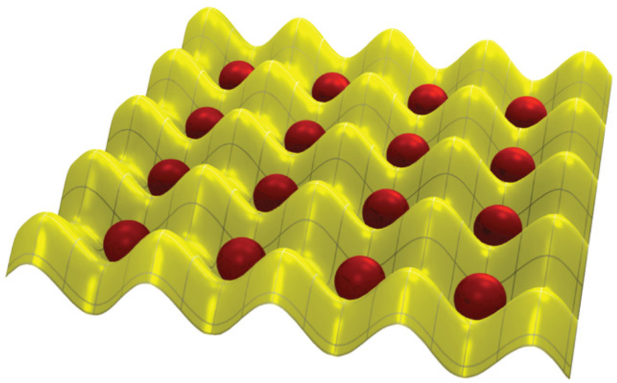

Trapped Neutral Atoms

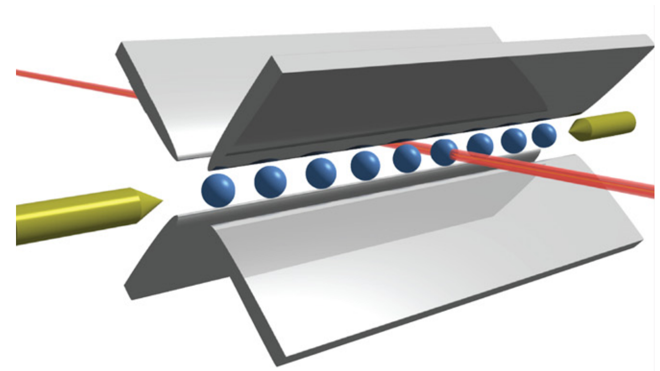

Trapped Ions

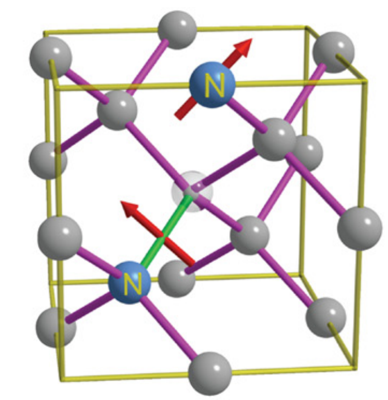

Nitrogen-Vacancy Centers

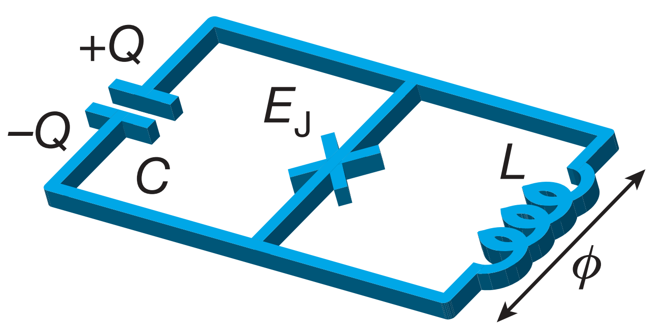

Superconductors

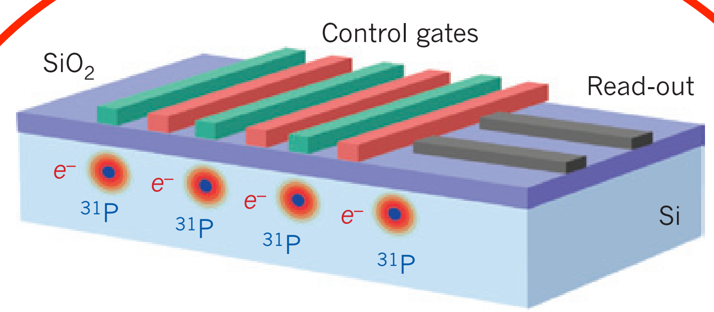

Donors in Solids

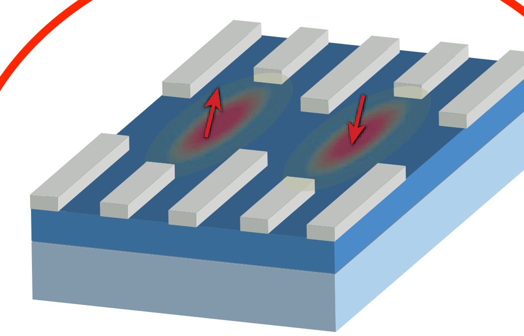

Quantum Dots

Images above are from the following references:

- I. Buluta, et al, *Natural and artificial atoms for quantum computation*, Rep. Prog. Phys. 74, 104401 (2011).
- T.D. Ladd et al, *Quantum computers*, Nature 464, 45 (2010).
- J.J.L. Morton et al, *Embracing the quantum limit in silicon computing*, Nature 479, 345 (2011).

Silicon-Based Spin Qubits

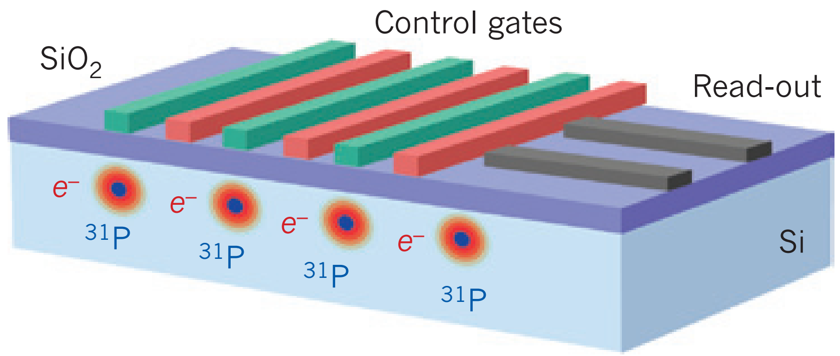

Considerations for silicon as a host material for spin qubits:

- Original proposal based on control of single donor qubits in silicon was published in B.E. Kane, Nature 393, 133 (1998).
- Spin-orbit interaction in silicon is relatively weak.
- Nuclear-spin-bearing isotope (^{29}Si) comprises only 5% of natural silicon and can be removed by isotopic enrichment.
- Advanced state of silicon technology offers a common platform for potential spin qubit integration with classical electronics.

Reference: J.J.L. Morton et al, *Embracing the quantum limit in silicon computing*, Nature 479, 345 (2011).

Sandia Silicon Device Description and Qubit Definition

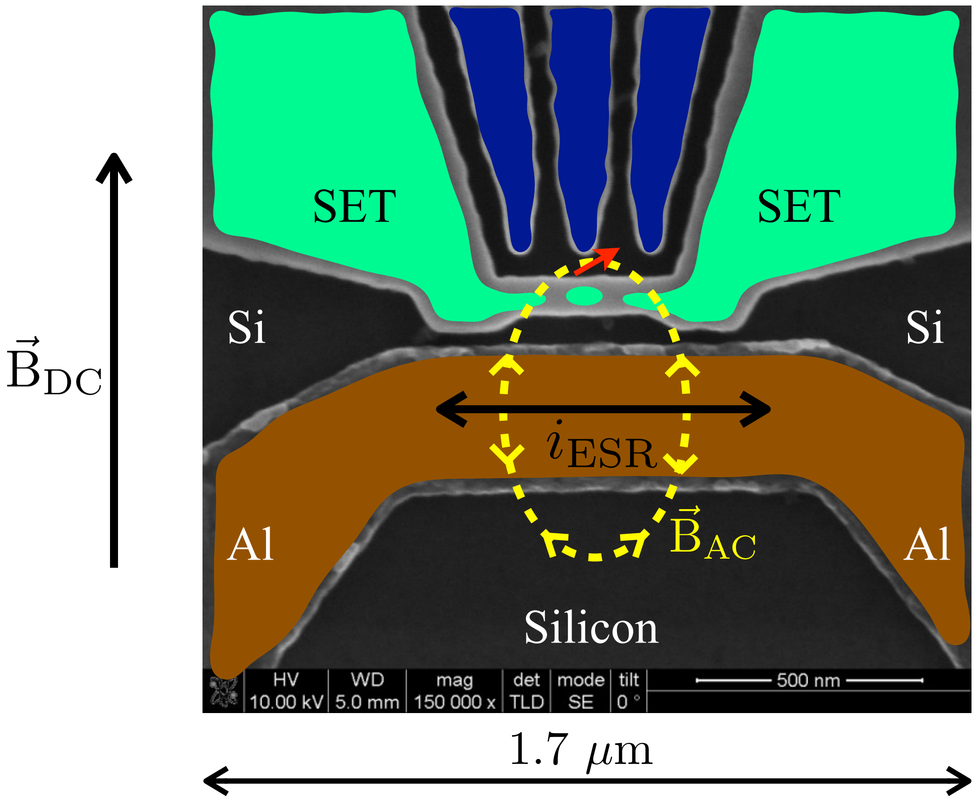

Top View of Silicon Device: SEM Image

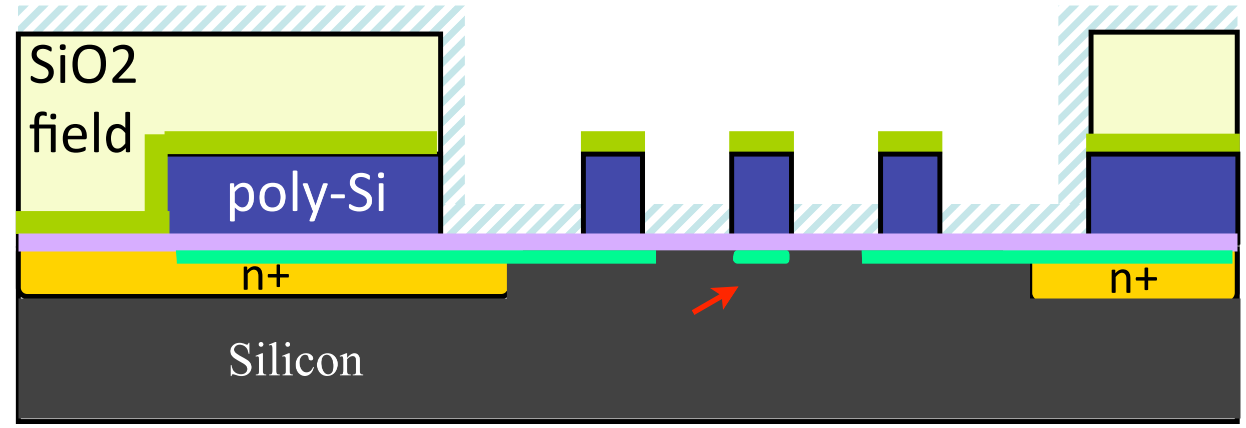

Schematic Cross-Sectional View of Silicon Device (ESR wire not shown)

- The regions in green have been electrostatically defined using the electrodes shown, resulting in the formation of a Quantum Dot or Single-Electron-Transistor (SET).

- At our ultra low temperature of operation, T = 15 mK, the electrons in the device can be at a different temperature, Te, than the substrate phonon bath at temperature T. For this particular device, we measured Te ≈ 300 mK for the electron temperature.

- An external static magnetic field $\vec{\mathrm{B}}_{\mathrm{DC}}$ of sufficient magnitude results in well-defined spin states |0> and |1> and enables spin-selective read-out using the SET.

- The Zeeman splitting is $\Delta\mathrm{E} = g\,\mu_B\,\mathrm{B}_{\mathrm{DC}} = h\,f_{\mathrm{ESR}}$. To avoid thermal smearing in spin read-out, the condition $\Delta\mathrm{E} > k_{\mathrm{B}}\mathrm{T}_{\mathrm{e}}$ must be satisfied.

- The measured electron temperature corresponds to:

$$\mathrm{T}_{\mathrm{e}} \approx 300\,\mathrm{mK} \Leftrightarrow 25\,\mu\mathrm{eV} \Leftrightarrow 6\,\mathrm{GHz} \Leftrightarrow 0.2\,\mathrm{T}$$

We perform Electron Spin Resonance (ESR) at $f_{\mathrm{ESR}} = 36\,\mathrm{GHz}$ and $|\mathrm{B}_{\mathrm{DC}}| = 1.3\,\mathrm{T}$

Therefore in our case: $\left(\frac{\Delta\mathrm{E}}{k_{\mathrm{B}}\mathrm{T}_{\mathrm{e}}}\right) \approx 6$

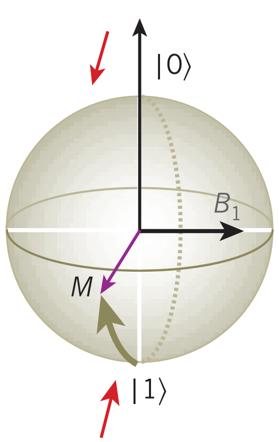

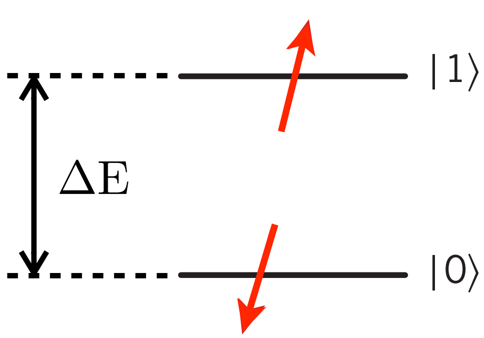

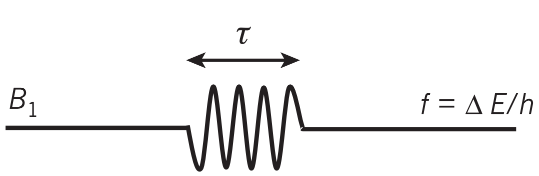

A Cryogenic Microwave Engineering Challenge

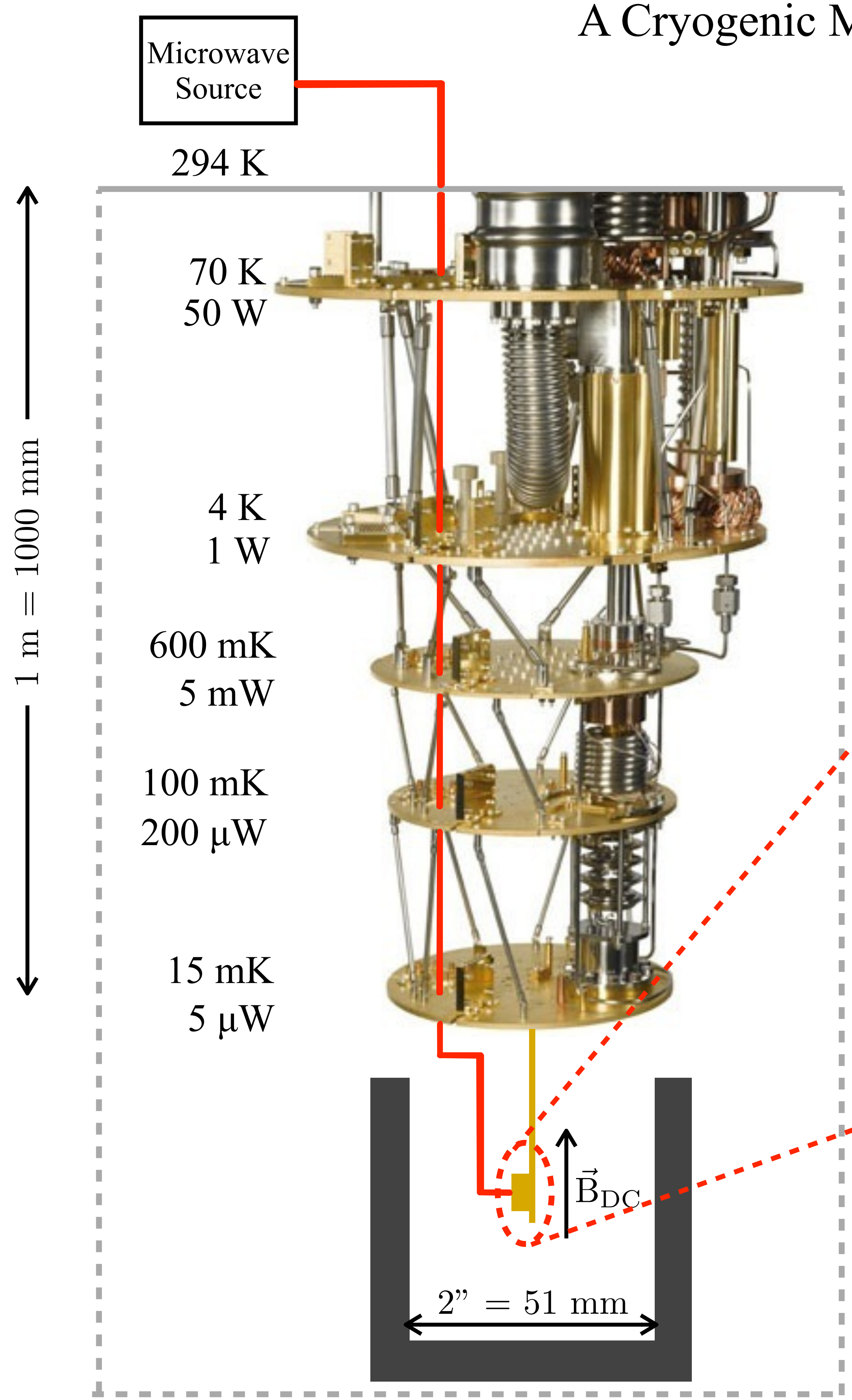

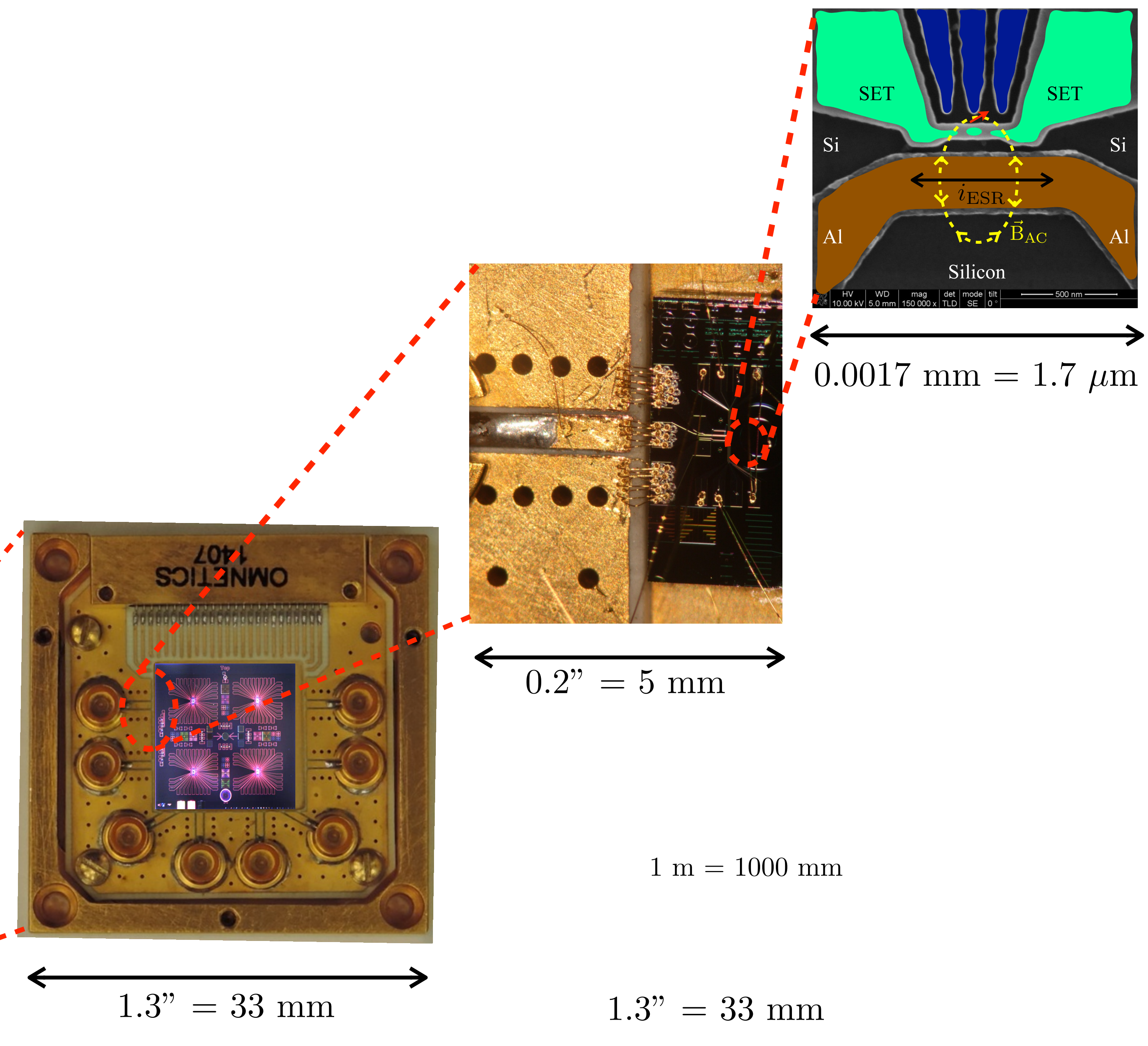

Image of dilution refrigerator stages from:
http://www.oxford-instruments.com/products/cryogenic-environments/

A Brief Introduction to Microwave Engineering

- The Electromagnetic Spectrum:

Radio-Frequency (RF) ranges from 30 MHz - 3 GHz corresponding to wavelengths of 10 m - 10 cm.

Microwave typically refers to 3 - 300 (GHz) corresponding to wavelengths of 10 cm - 1 mm.

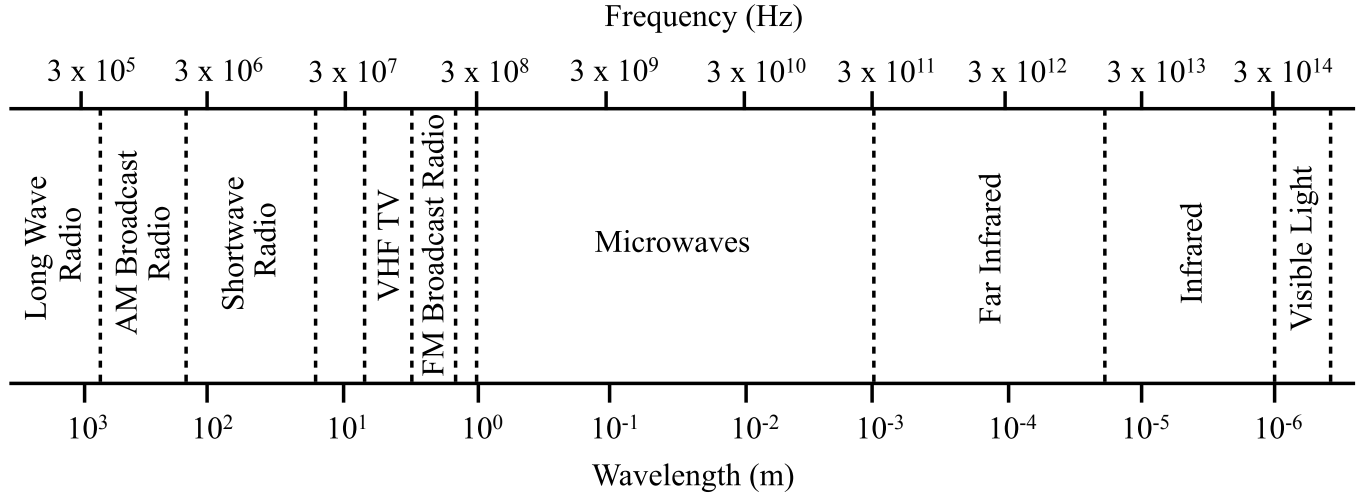

- Maxwell's Equations: $\nabla \times \vec{\mathrm{E}} = -\frac{\partial \vec{\mathrm{B}}}{\partial t} - \vec{\mathrm{M}},$ $\quad \nabla \times \vec{\mathrm{H}} = \frac{\partial \vec{\mathrm{D}}}{\partial t} + \vec{\mathrm{J}},$ $\quad \nabla \cdot \vec{\mathrm{D}} = \rho,$ $\quad \nabla \cdot \vec{\mathrm{B}} = 0$

- Microwave Engineering: Utilizes both field theory and extended circuit theory toward diverse applications. Consider an example:

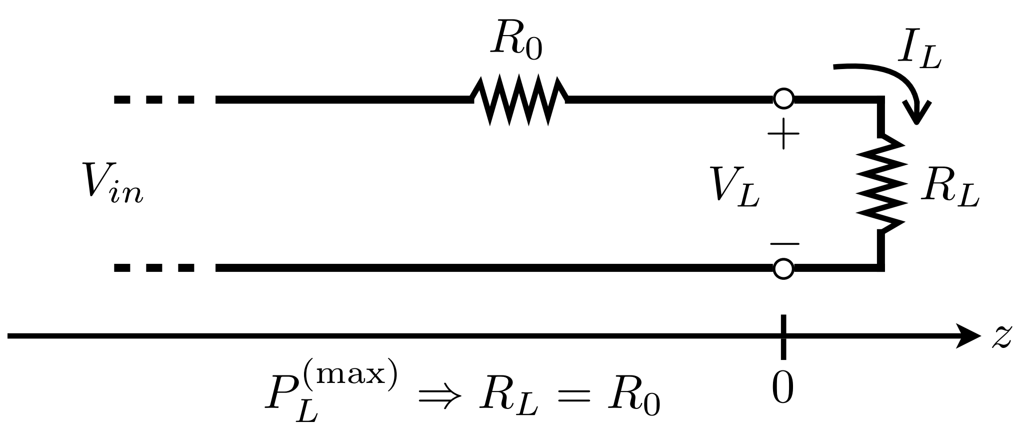

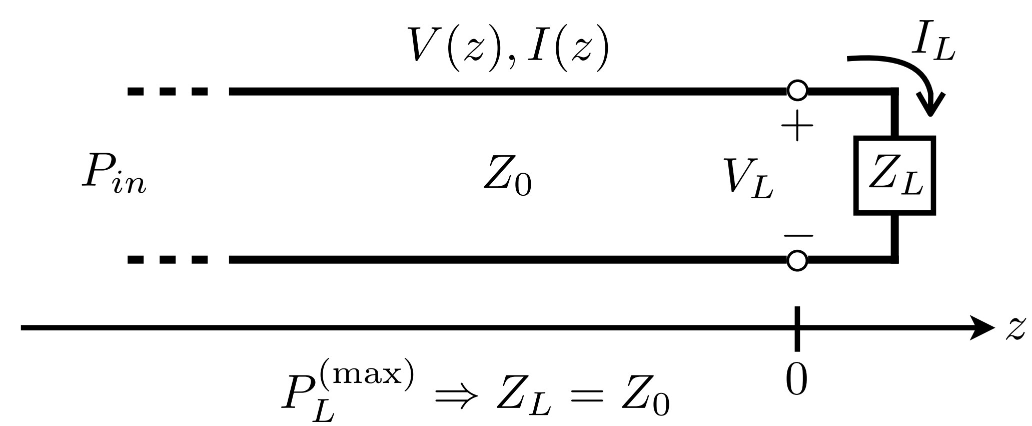

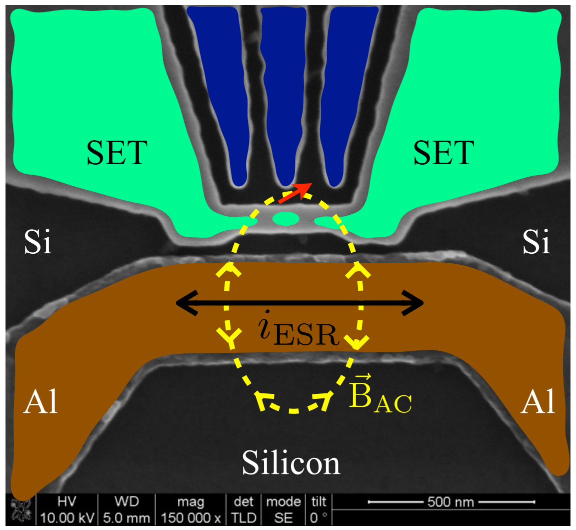

- For our experiments we want to maximize the local AC magnetic field and therefore maximize the *current* through the load.:

$$\mathrm{B}_{\mathrm{AC}} = c \cdot i_{\mathrm{ESR}}$$

$$P_{in} = \frac{1}{8}\left(1 - |\Gamma|^2\right) i_{\mathrm{ESR}}^2\, Z_0$$

$$\Rightarrow P_{in} = \frac{1}{8c^2}\left(1 - |\Gamma|^2\right) Z_0\, \mathrm{B}_{\mathrm{AC}}^2$$

Electromagnetic Field Simulation: Description

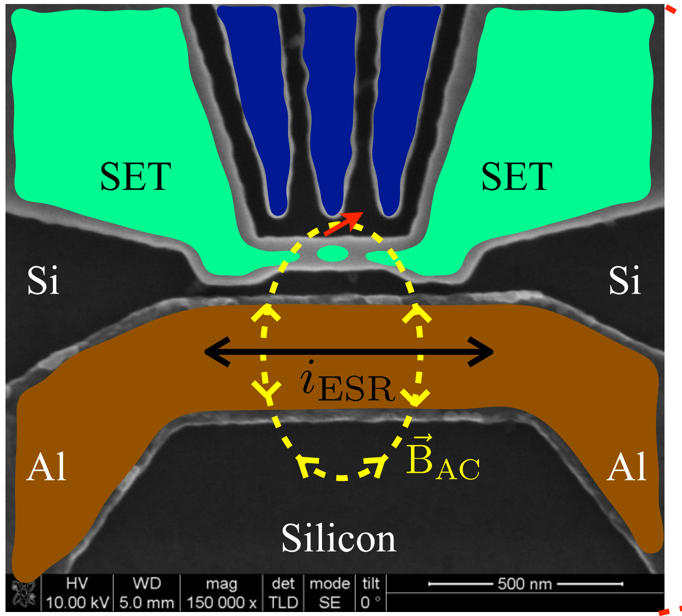

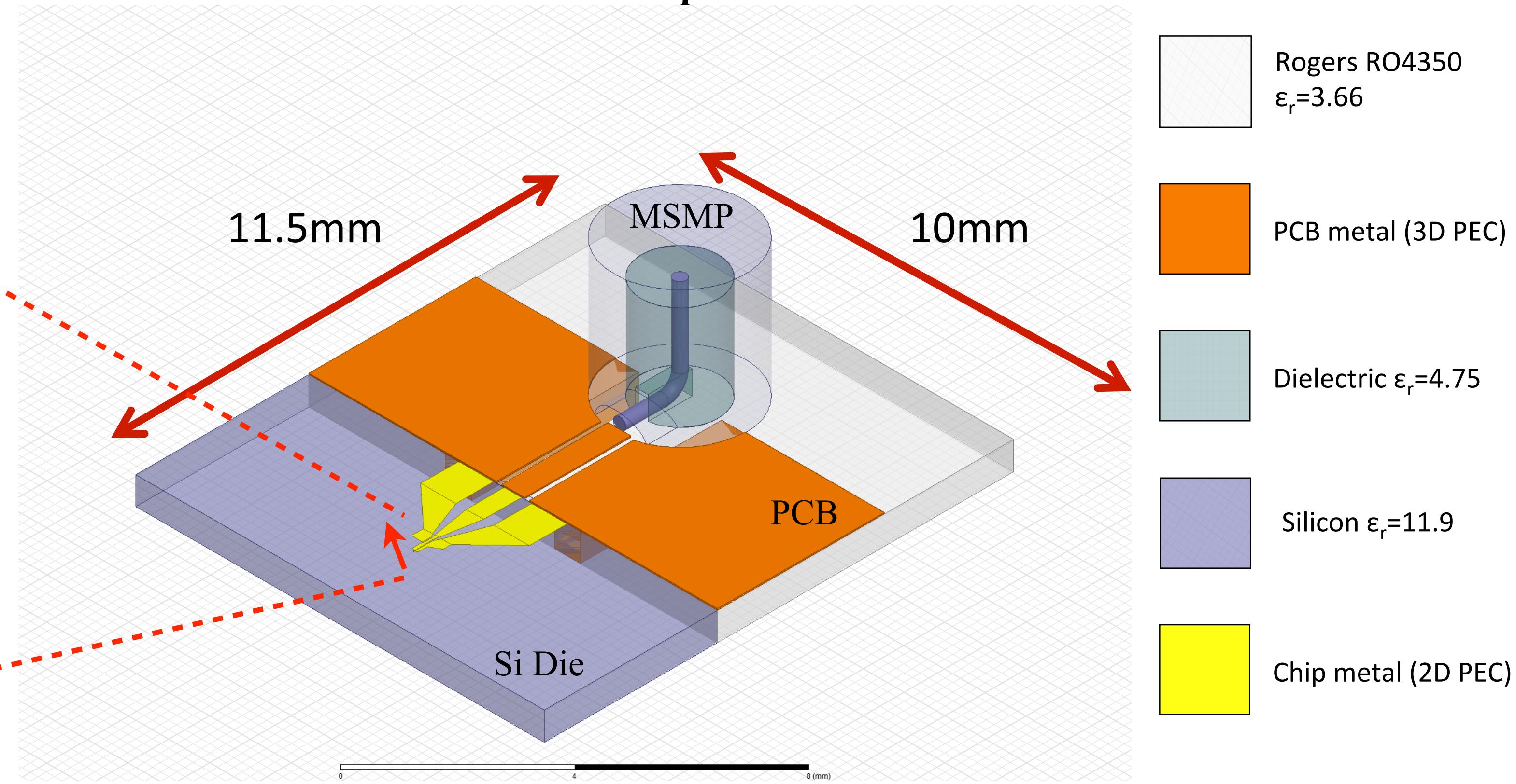

Entire solid model that was simulated using HFSS. Key on right.
Acknowledgement: John Borchardt, Sandia National Laboratories

- "MSMP" in simulated structure above is right angle coaxial-to-PCB Mini-SMP µwave connector.

- "PCB" in simulated structure above (orange) is Printed Circuit Board.:

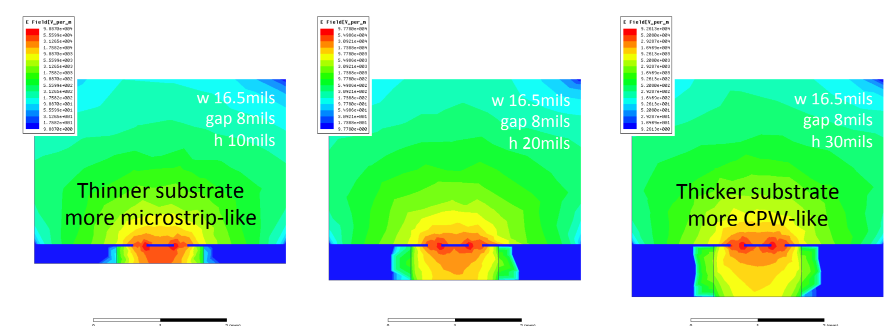

- On-Chip Transmission Line: Colored yellow and labeled "Si Die" in simulated structure above:
  - On-chip transmission line design from CQCCT and described in J.P. Dehollain et al, Nanotechnology 24, 015202 (2013).
  - The on-chip transmission line includes CPW to CPS transition (balun). CPW = CoPlanar Waveguide, CPS = CoPlanar Stripline.
  - Wire bonds not modeled but impact expected to be minimal due to CPW mode design. Our PCB-to-Chip transition shown above.

Electromagnetic Field Simulation: Results

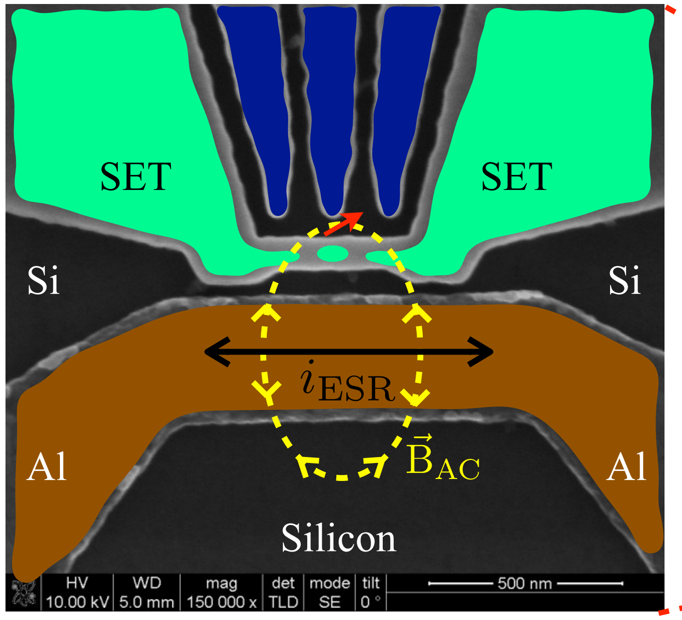

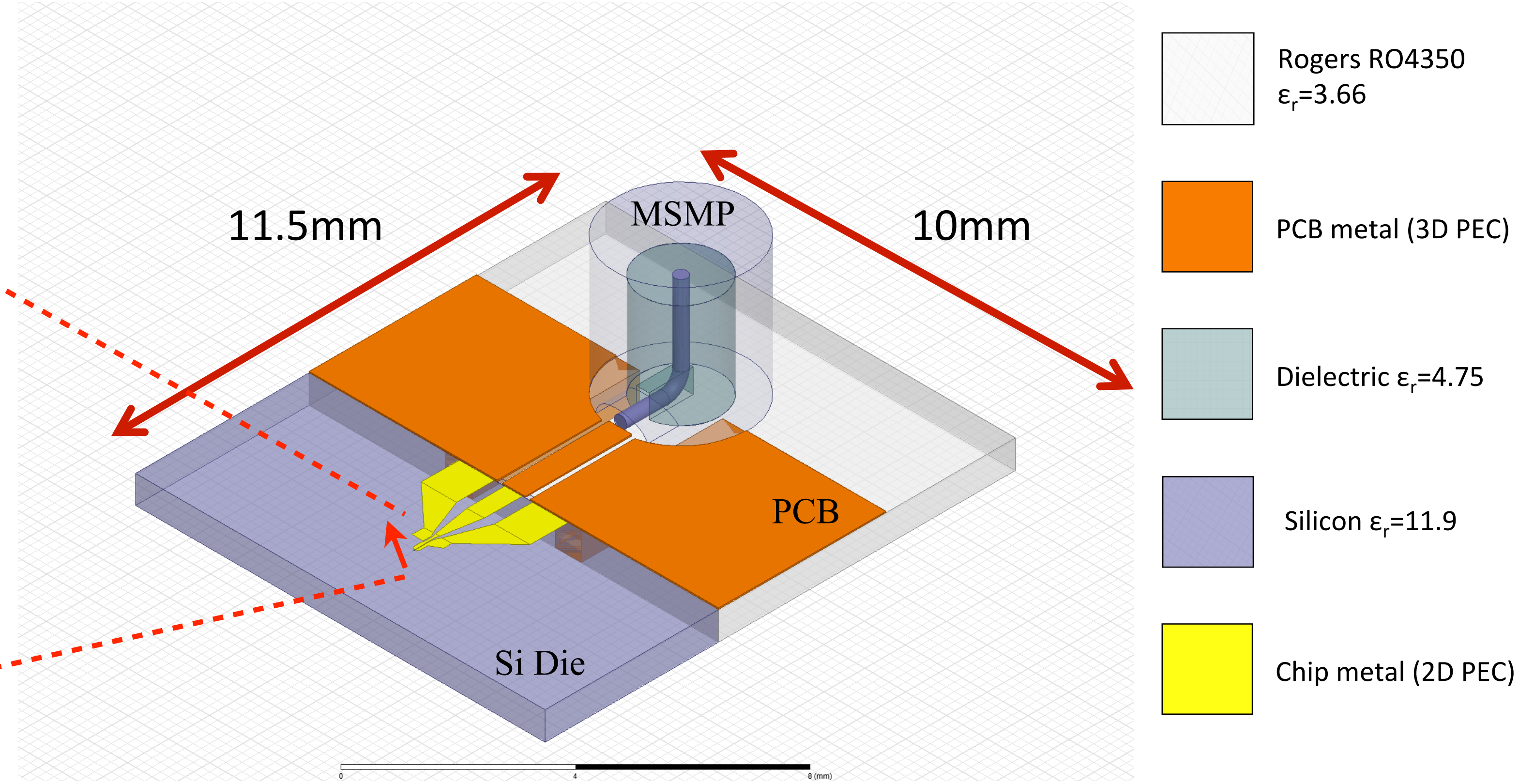

Entire solid model that was simulated using HFSS. Key on right.

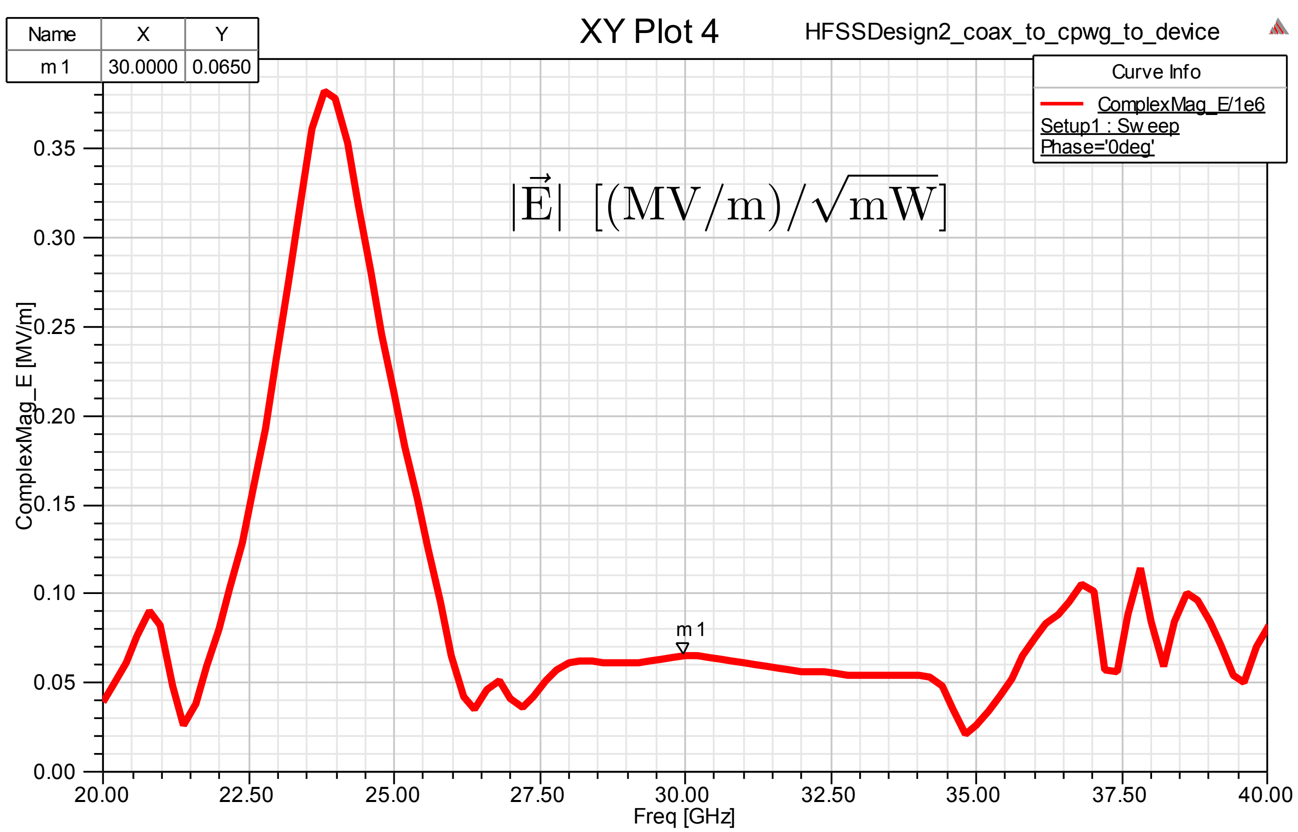

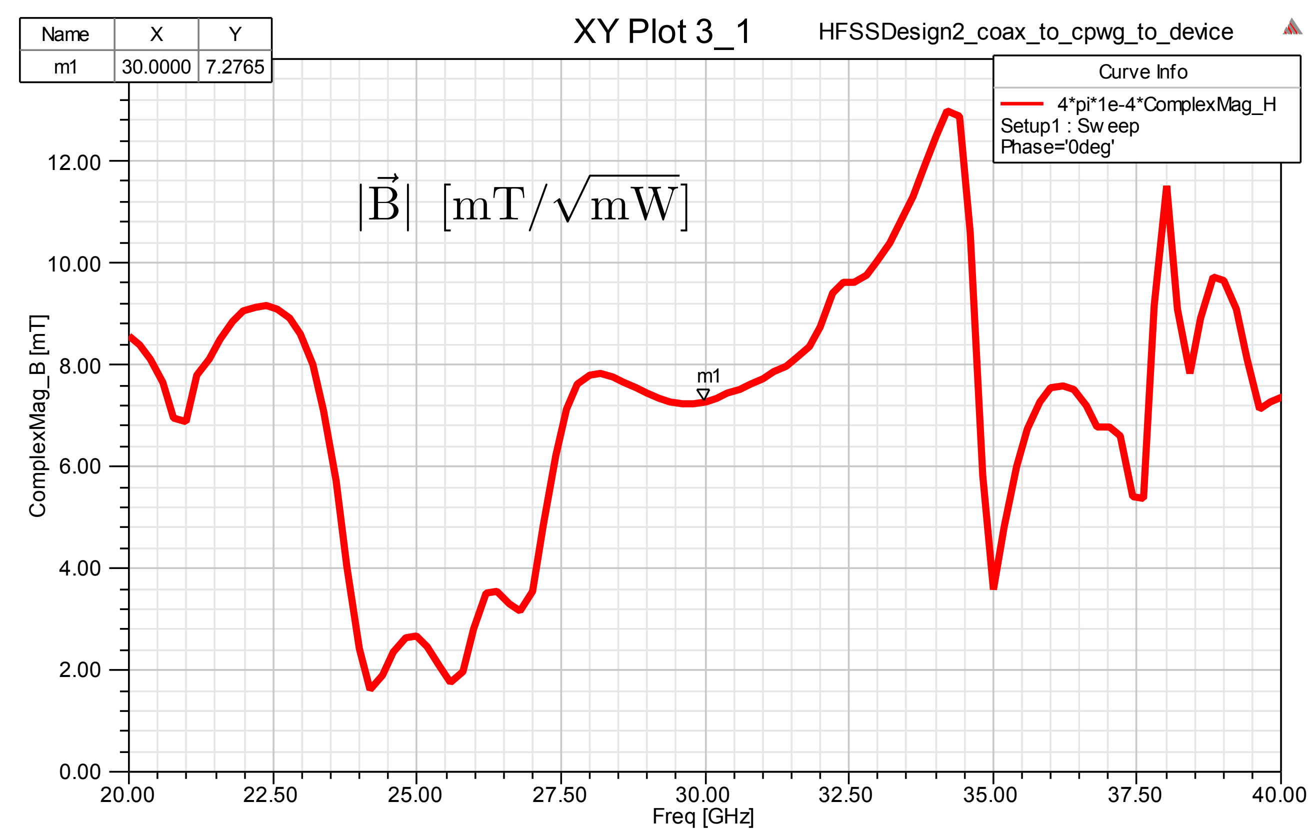

Experimental Data for the Silicon Device: Coulomb Blockade

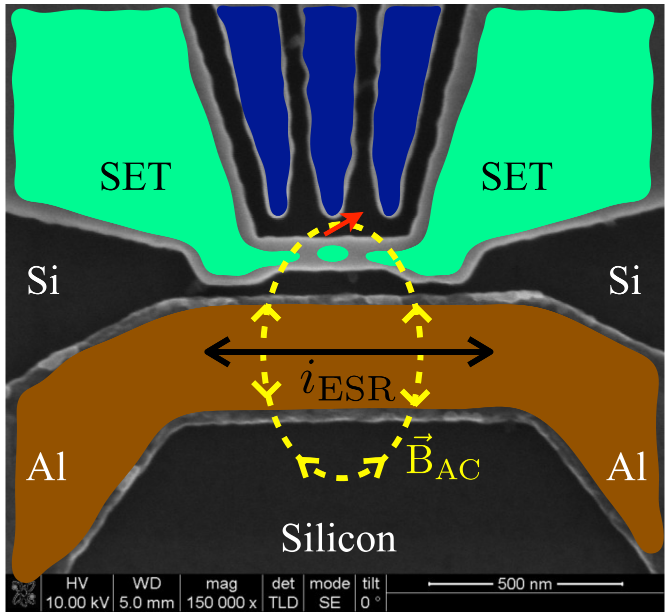

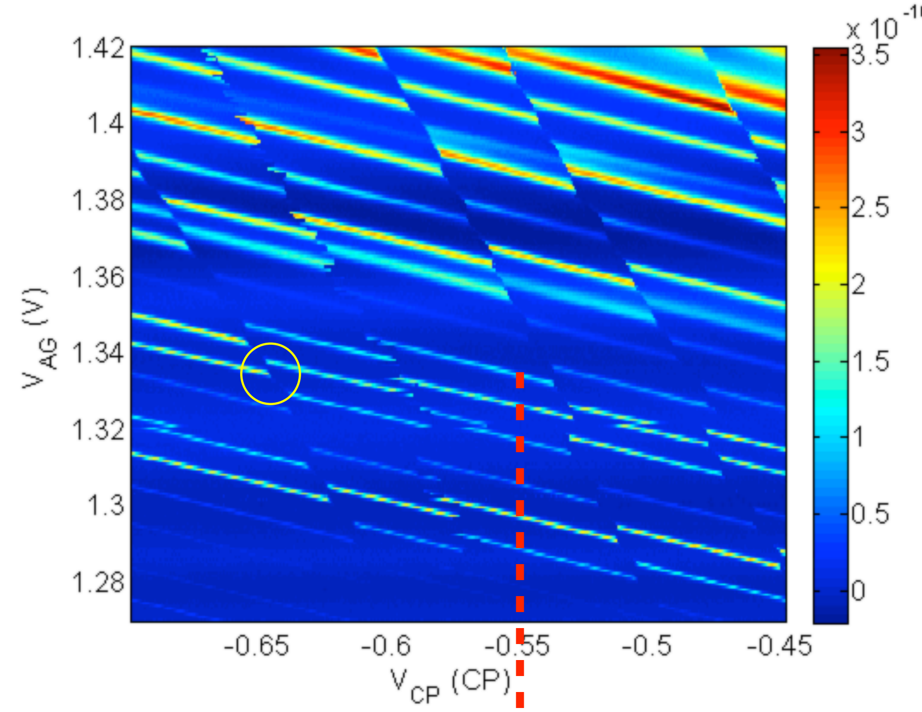

Dwight Luhman et al,
Sandia National Laboratories

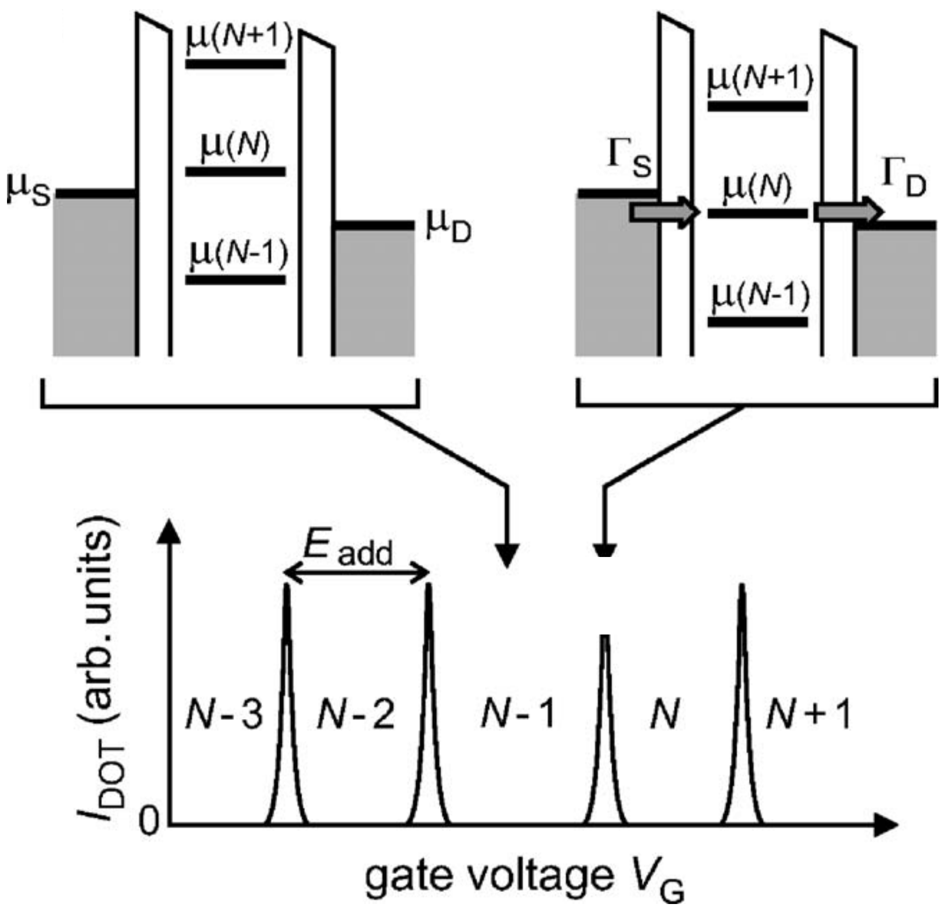

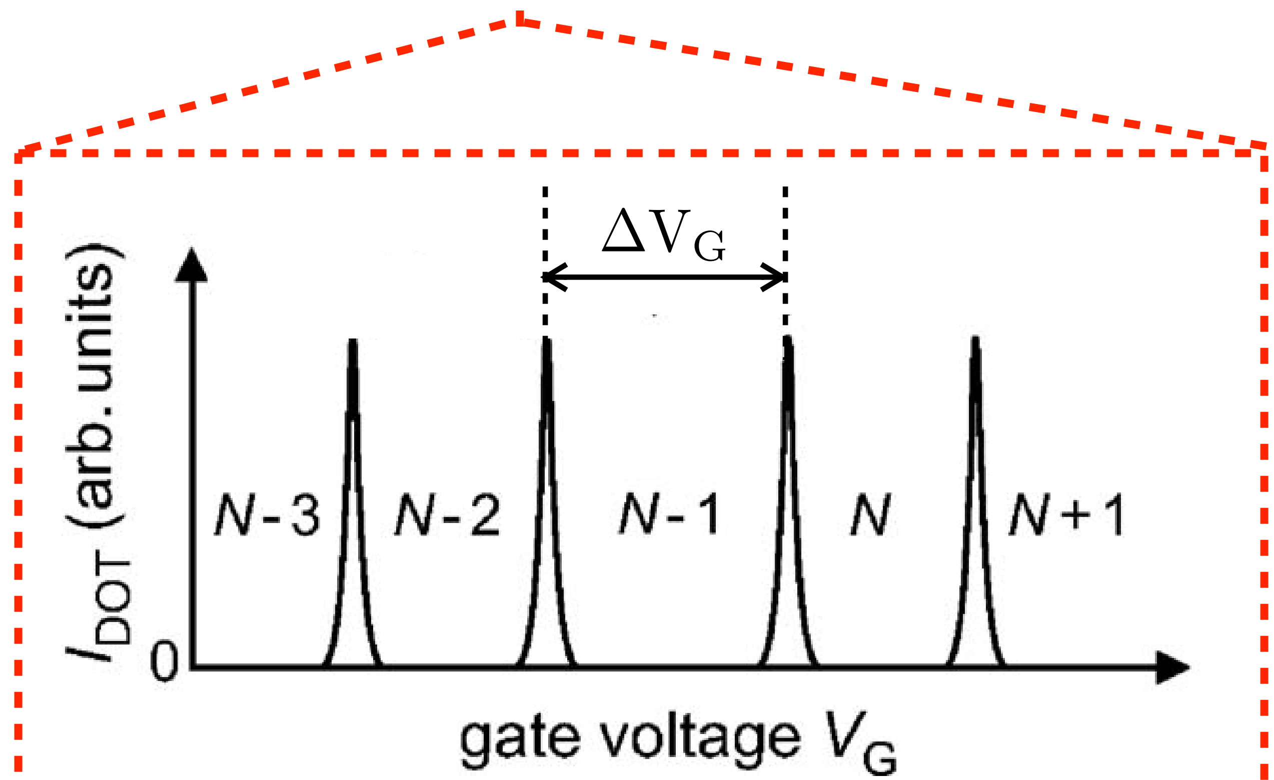

Coulomb Blockade

Experimental Data for the Silicon Device: Spin Read-Out

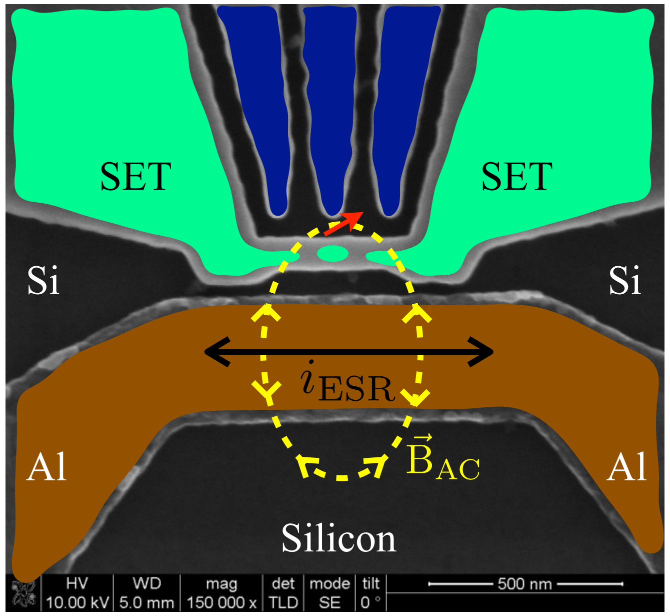

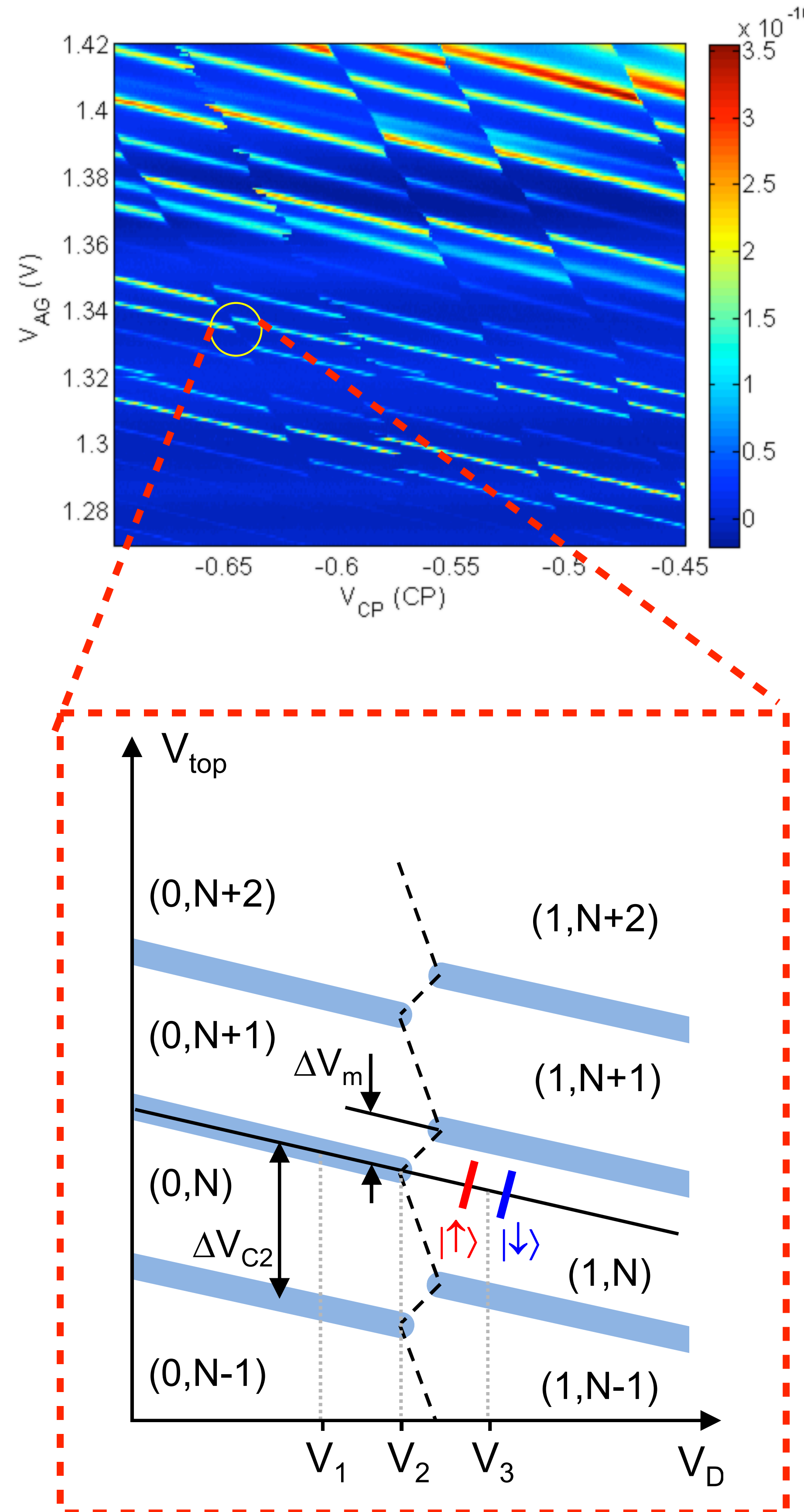

Dwight Luhman et al,
Sandia National Laboratories

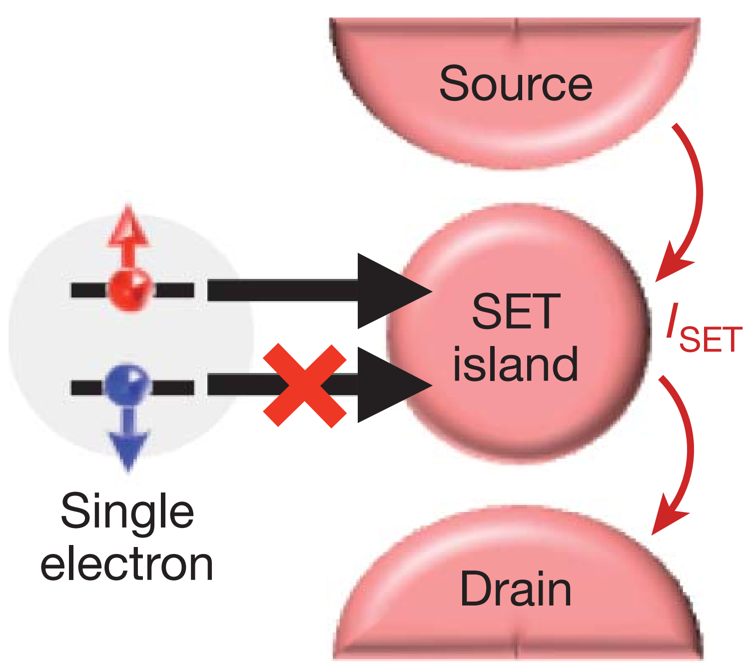

A. Morello, et al, Nature 467, 687 (2010)

A. Morello, et al,
Physical Review B
80, 081307 (2009)

Experimental Data for the Sandia Silicon Device

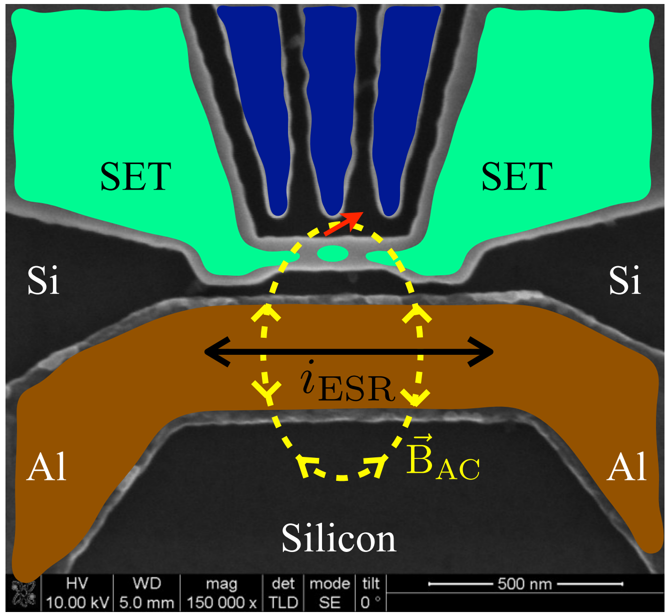

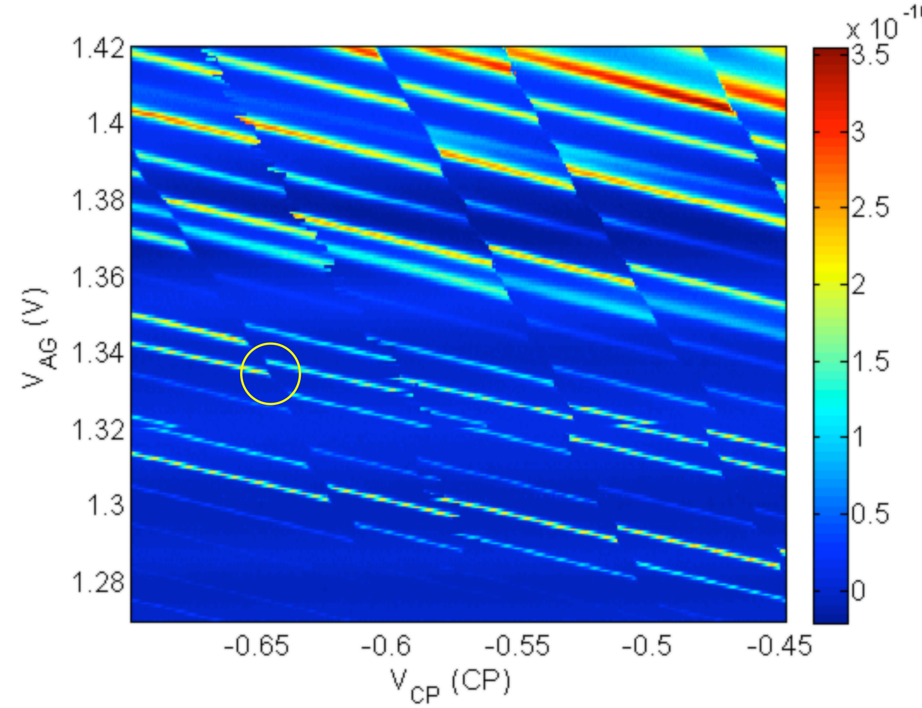

Dwight Luhman et al,
Sandia National Laboratories

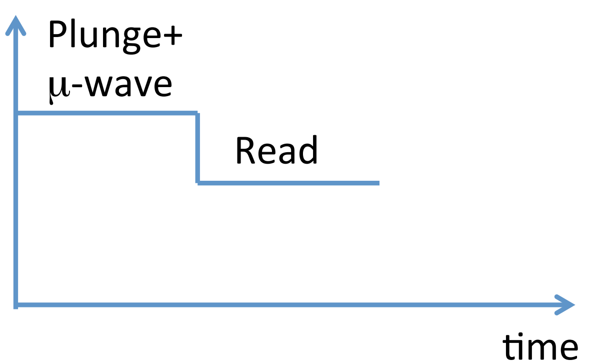

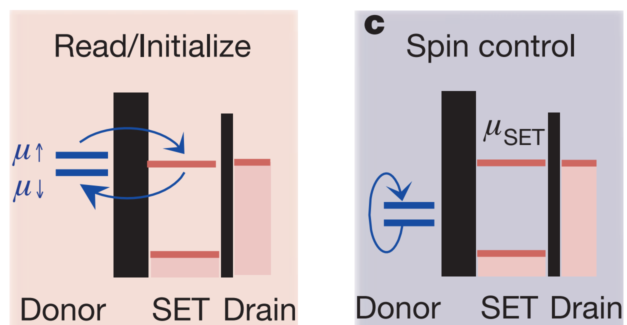

J.J. Pla et al, Nature 489, 541 (2012)

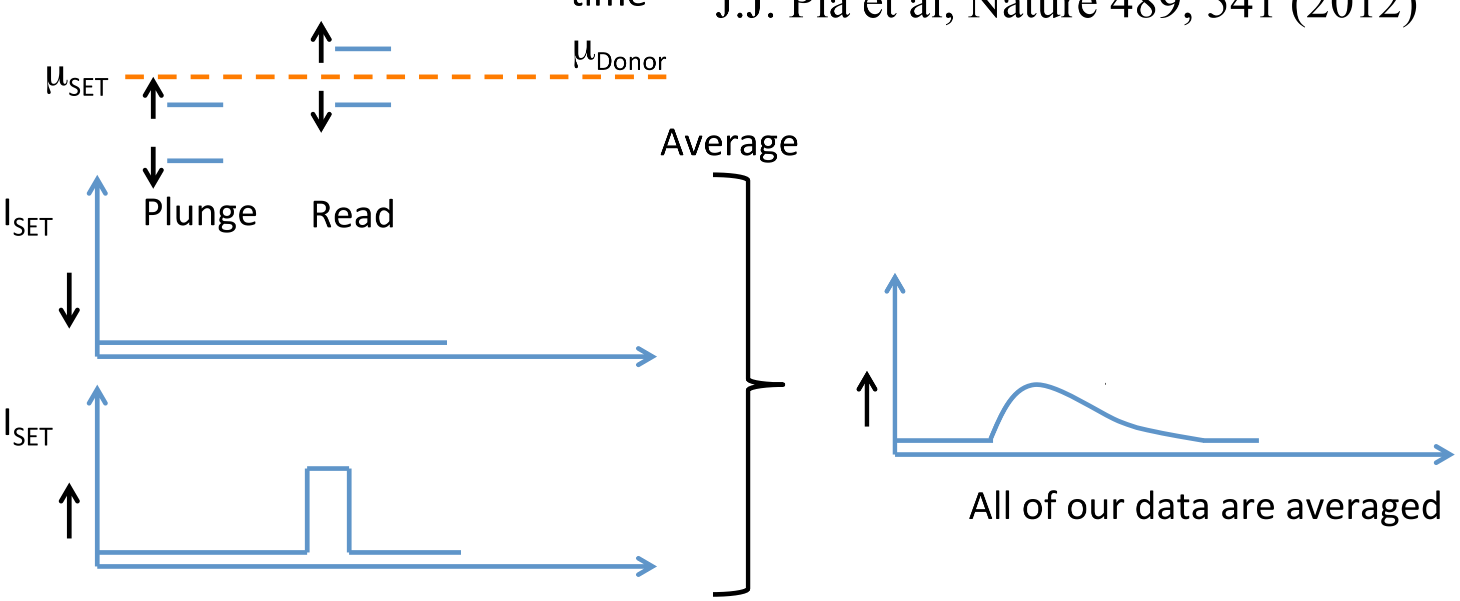

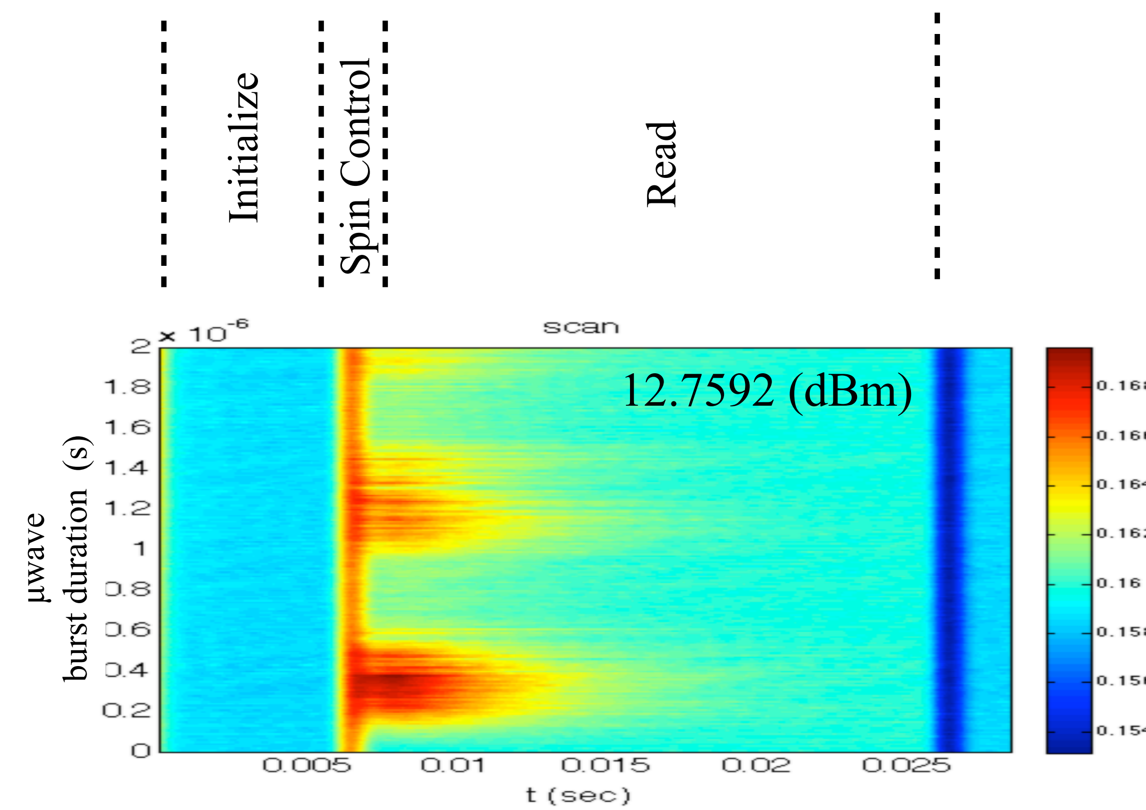

Dwight Luhman et al, Sandia National Laboratories

Sandia Silicon Device: Experimental Rabi Oscillations

Dwight Luhman et al,
Sandia National Laboratories

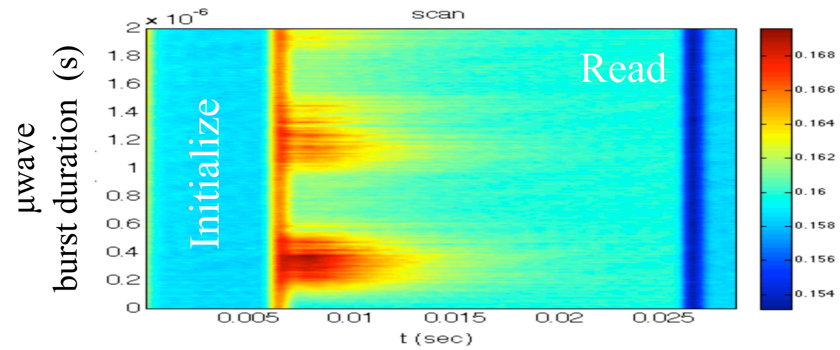

12.7592 (dBm)

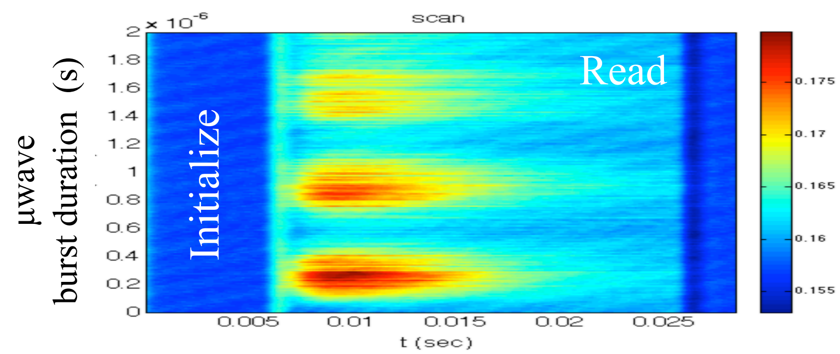

15.5929 (dBm)

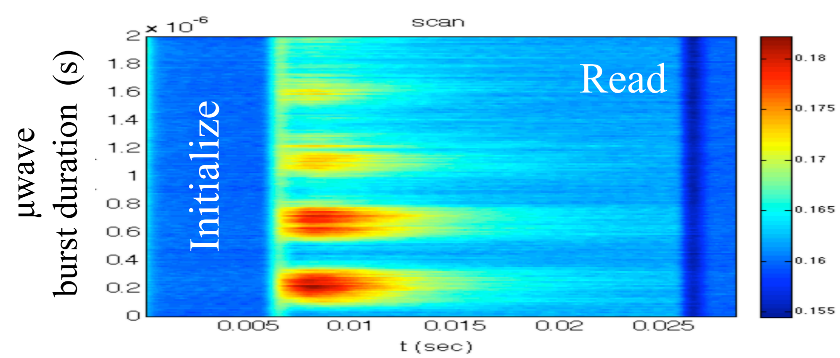

18.0320 (dBm)

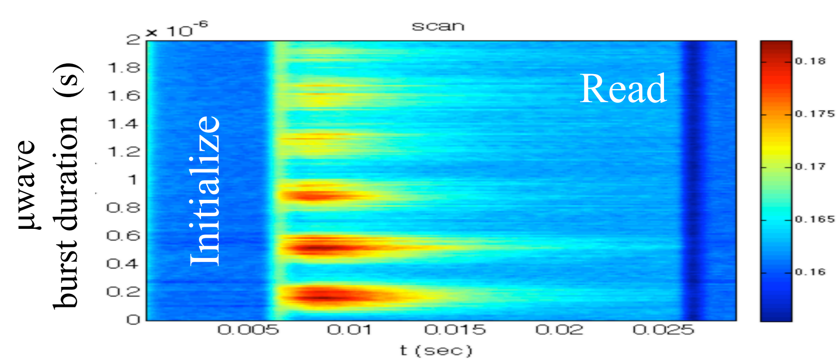

20.4525 (dBm)

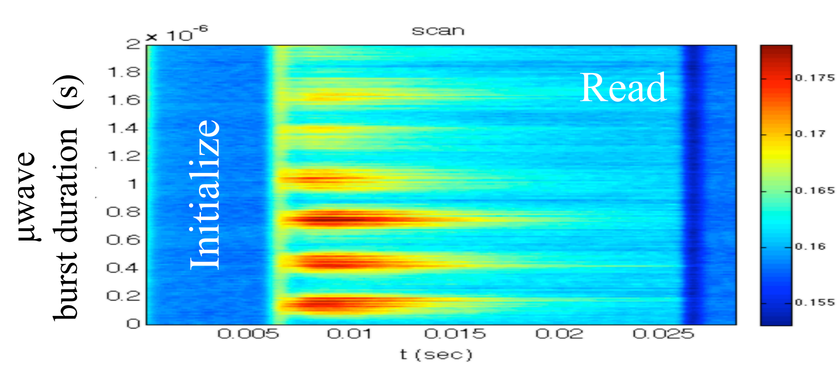

22.1363 (dBm)

Sandia Silicon Device: Experimental Rabi Oscillations

Dwight Luhman et al,
Sandia National Laboratories

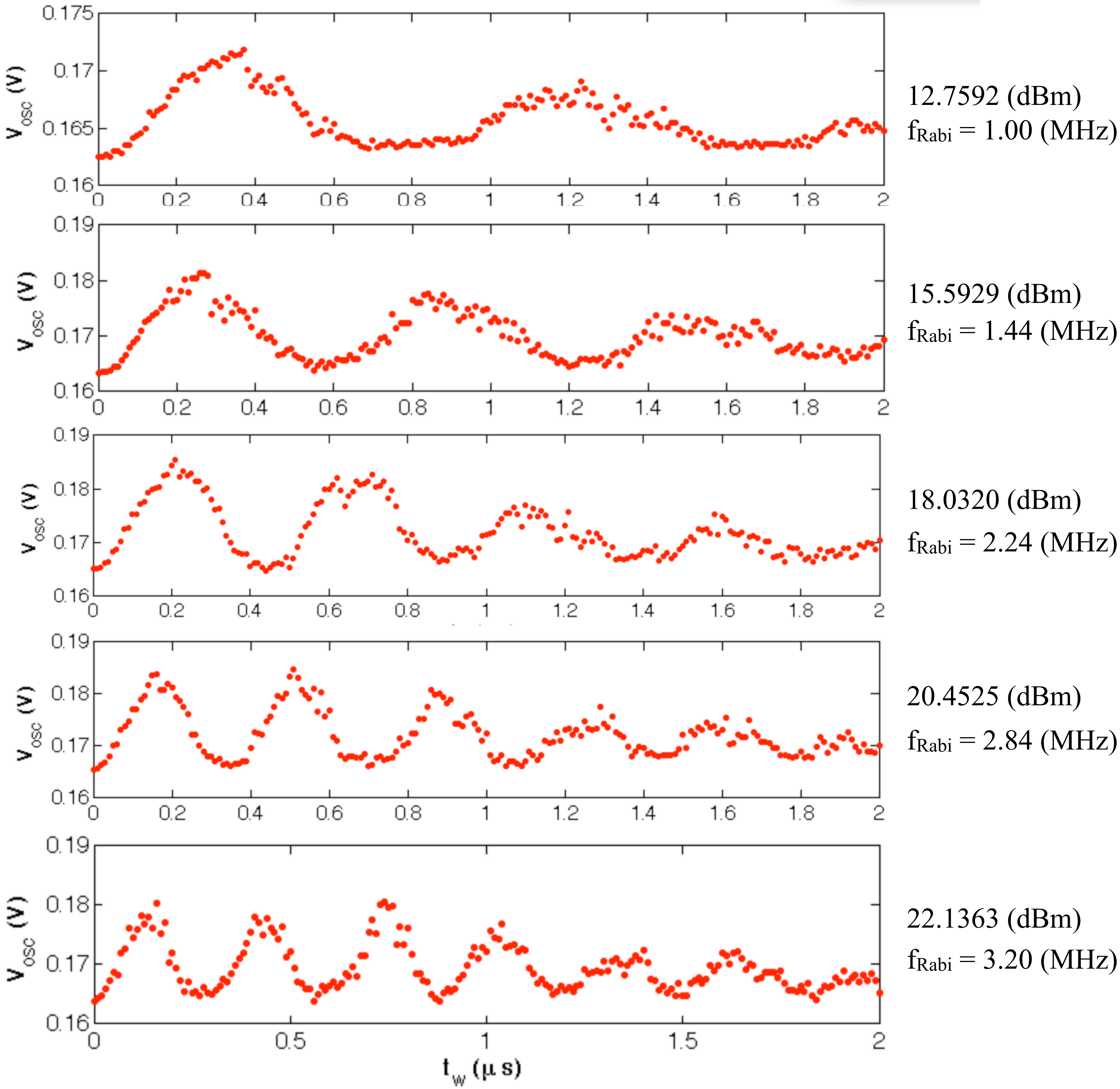

Rabi Frequency and AC Magnetic Field Dependence on Applied μwave Power

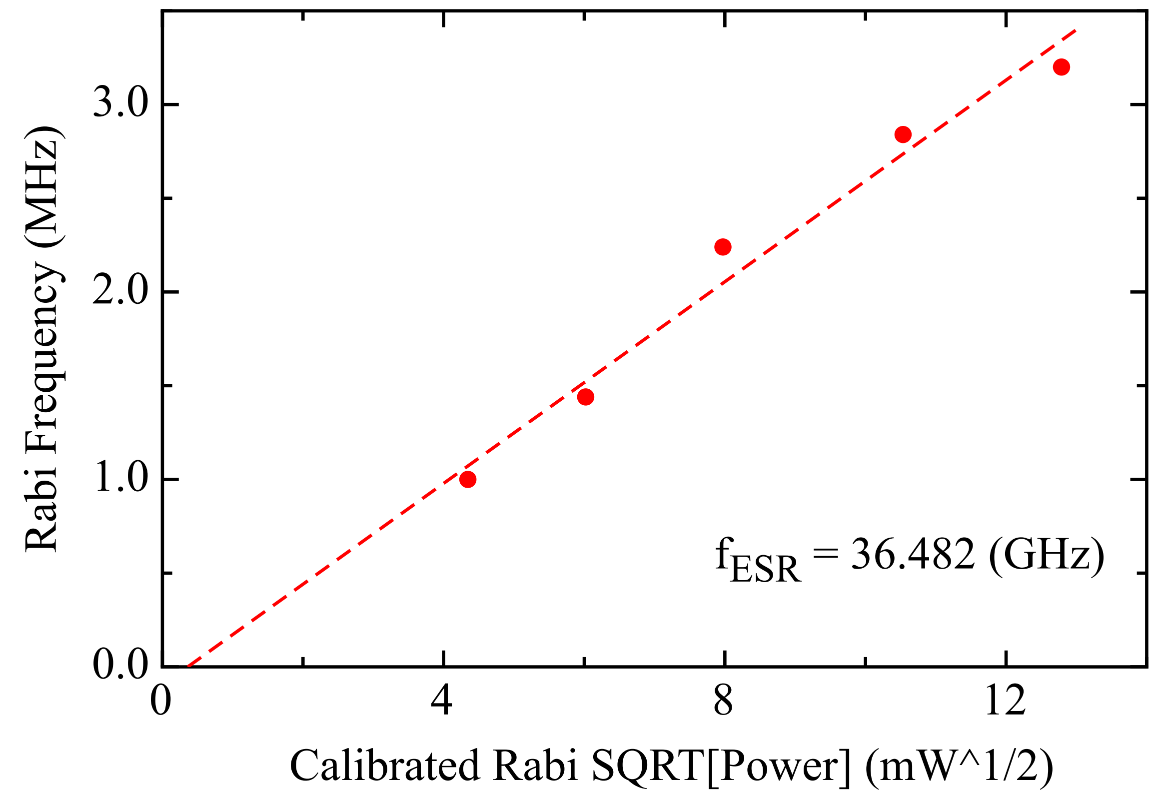

$$\omega_{\rm Rabi} = \frac{1}{2}\sqrt{(\omega-\omega_0)^2 + (V_{ab}/\hbar)^2}$$

$$V_{ab} \equiv < \psi_a | V | \psi_b >$$

Here the driving amplitude is proportional to the AC magnetic field thus:

$$f_{\rm Rabi} \equiv \omega_{\rm Rabi}/2\pi = \frac{1}{2} g\, \mu_B\, B_{\rm ac}/h$$

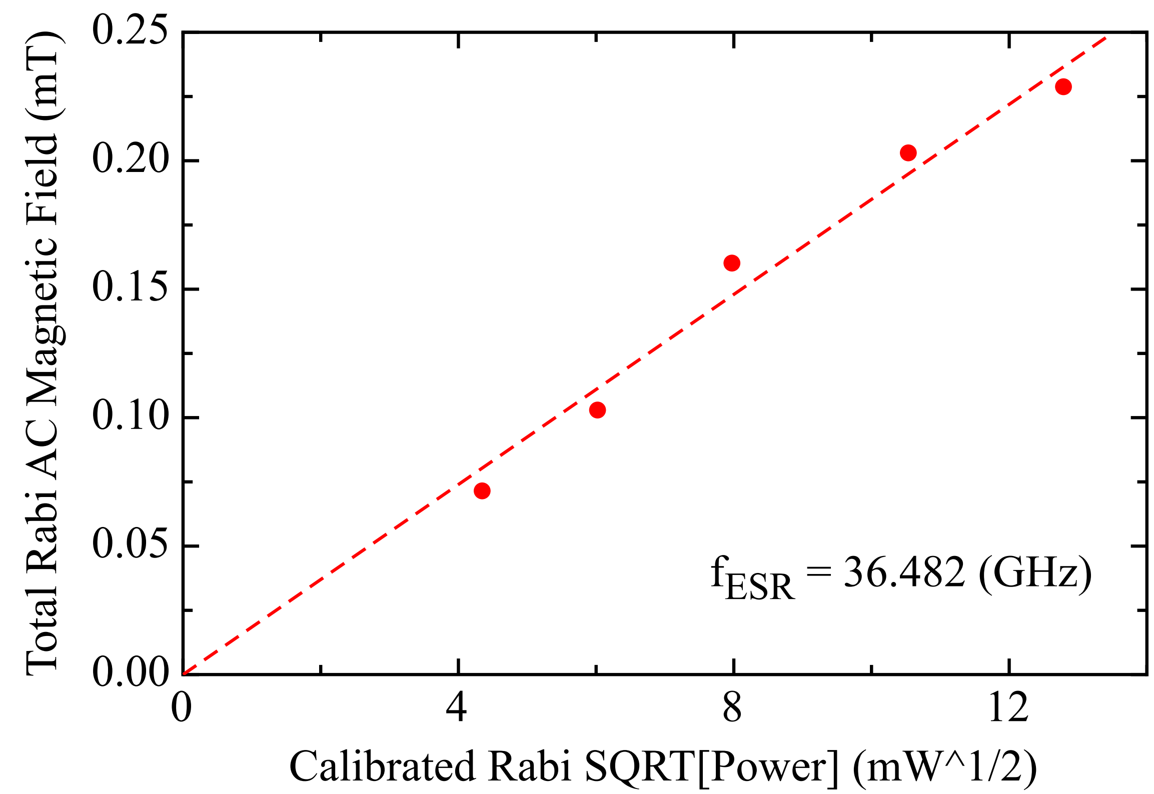

Normalized AC Magnetic Field: Comparison Between Experiment and Simulation

Using the calibrated source power and the AC magnetic field extracted from the experimental Rabi frequencies, we can extract the 'normalized' AC magnetic field shown in the plot [0.0185 (mT/√mW)] at f_{ESR} = 36.482 (GHz).

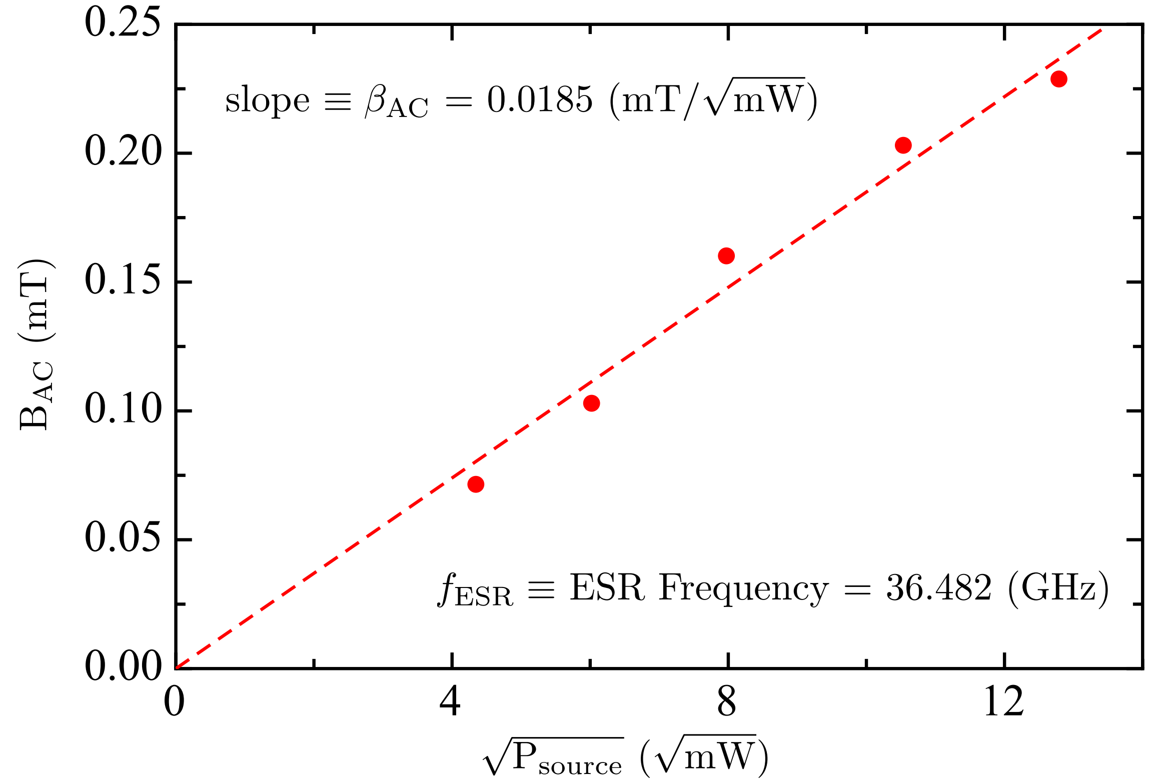

$$B_{AC} = c \cdot i_{ESR} \quad P_{in} = \frac{1}{8}(1 - |\Gamma|^2)\, i_{ESR}^2\, Z_0$$

$$\Rightarrow P_{in} = \frac{1}{8c^2}(1 - |\Gamma|^2)\, Z_0\, B_{AC}^2$$

$$\beta_{AC} \equiv \frac{B_{AC}\ (\mathrm{mT})}{\sqrt{P_{source}}\ (\sqrt{\mathrm{mW}})} = \sqrt{\alpha} \cdot \left[\frac{B_{AC}\ (\mathrm{mT})}{\sqrt{P_{MSMP}}\ (\sqrt{\mathrm{mW}})}\right]$$

$$\text{slope} \equiv \beta_{AC} = 0.0185\ (\mathrm{mT}/\sqrt{\mathrm{mW}})$$

From the table on the right: 42 < α (dB) < 52

$$2\ (\mathrm{mT}/\sqrt{\mathrm{mW}}) < \left[\frac{B_{AC}\ (\mathrm{mT})}{\sqrt{P_{MSMP}}\ (\sqrt{\mathrm{mW}})}\right] < 7\ (\mathrm{mT}/\sqrt{\mathrm{mW}})$$

Component	**Approximate Loss at 36.482 GHz (dB)**
RF Switch	6
RT Cable	5
Cryogenic Coaxial Cable: RT to MSMP PCB	30 - 35
Total Attenuation from Attenuators	1 - 6
TOTAL from RF Source at RT to MSMP R/A PCB	42 - 52

Normalized AC Magnetic Field: Comparison Between Experiment and Simulation

Experiment: $2\ (\mathrm{mT}/\sqrt{\mathrm{mW}}) < \left[\frac{B_{AC}\ (\mathrm{mT})}{\sqrt{P_{MSMP}}\ (\sqrt{\mathrm{mW}})}\right] < 7\ (\mathrm{mT}/\sqrt{\mathrm{mW}})$

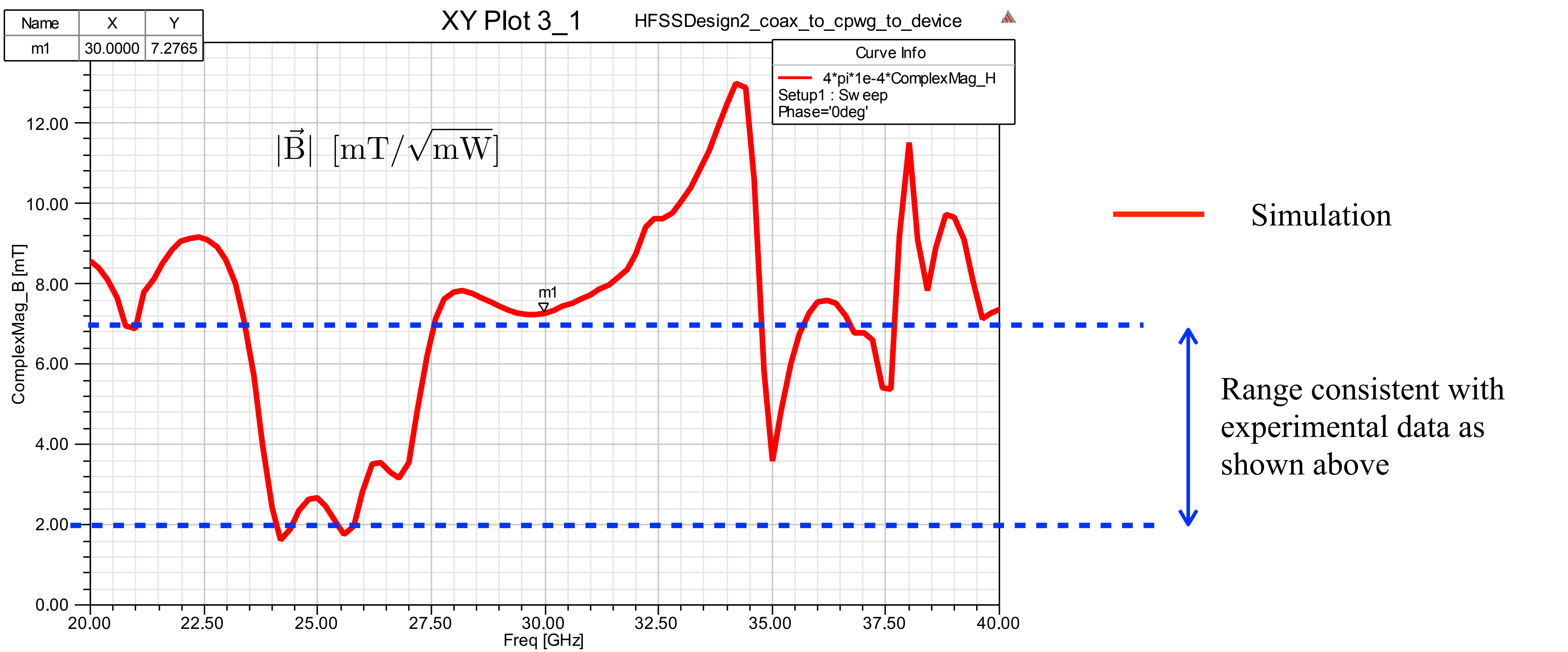

Sandia National Laboratories

Conclusions

- State-of-the-Art Physics often requires state-of-the-art techniques and engineering, as was the case for the work presented.
- A central challenge for this work was delivering a strong microwave magnetic field to the single spin location.
- This central challenge was addressed through careful microwave design that included 3D electromagnetic field simulation.
- Our experimental data reveals coherent Rabi oscillations of a single electron spin.
- Reasonable agreement was found between the experimental data and the electromagnetic field simulation.

Progress of joint UNM-SNL effort toward achieving state-of-the-art read-out using cryogenic preamplification

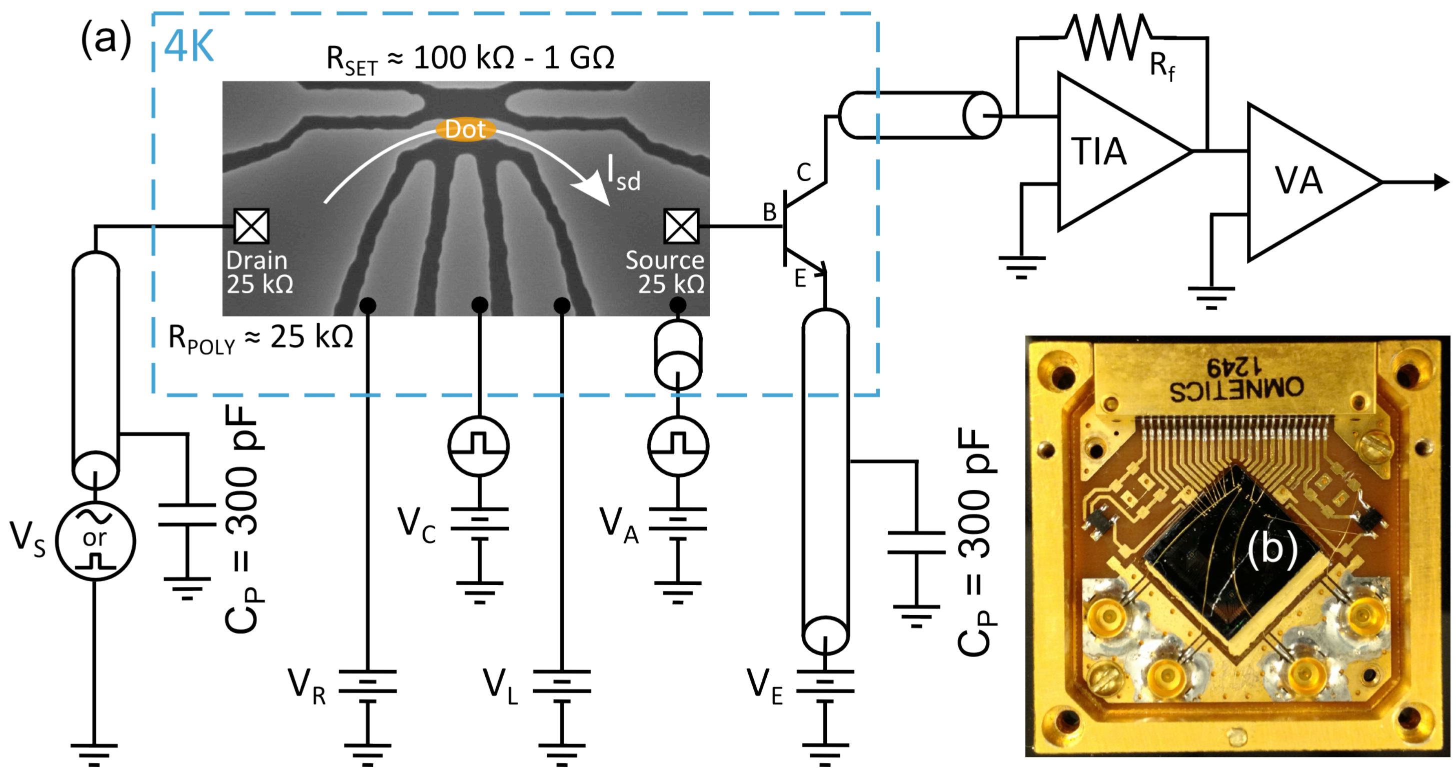

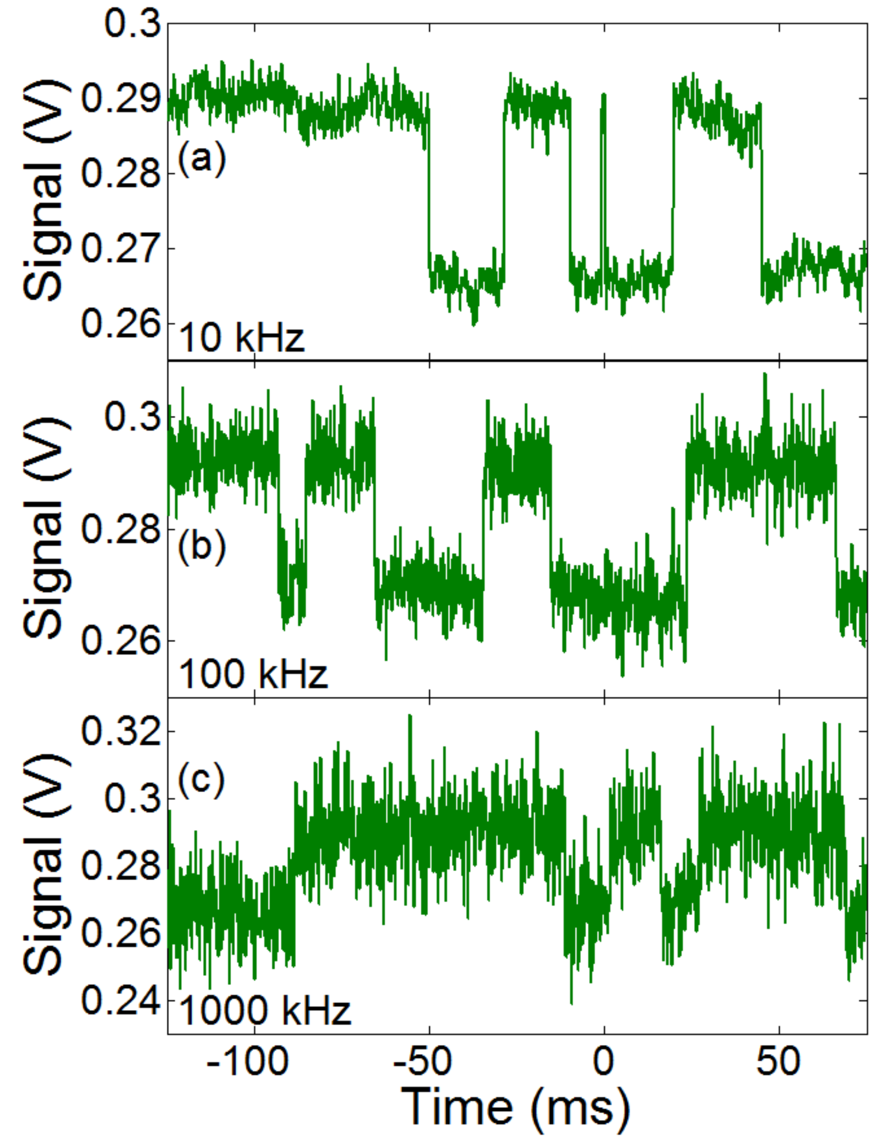

Matt Curry, CQuIC at UNM and Sandia National Laboratories (manuscript in preparation).

Acknowledgements

Quantum Information Science and Technology (QIST) at Sandia National Laboratories

Principal Investigator: Malcolm Carroll

ESR Fabrication:

- L.A. Tracy
- N. Bishop
- T. Pluym
- J. Wendt
- G. Ten Eyck
- M.P. Lilly

ESR Microwave Design and Cryogenic Hardware:

- J. Borchardt
- S.M. Carr

ESR Measurement:

- D.R. Luhman
- K. Nguyen
- L.A. Tracy
- M.P. Lilly

Joint Research Efforts with the External Community

- Center for Quantum Information and Control (CQuIC) at University of New Mexico (M.J. Curry and I. Deutsch)
- Australian Centre for Quantum Computing and Communication Technology (CQCCT) (A. Dzurak, L. Hollenberg, D. Jamieson, A. Morello, S. Rogge, M. Simmons)
- Princeton University (S. Lyon)
- NIST (N. Zimmerman)
- U. Maryland (S. Das Sarma)
- National Research Council (A. Sachrajda)
- U. Sherbrooke (P. Harvey-Collard, C. Bureau-Oxton, M. Pioro-Ladriere)
- Purdue University (G. Klimeck & R. Rahman)
- U. Wisconsin (M. Eriksson, M. Friesen)